1352
doi:10.1017/S1431927622005530
Microsc. Microanal. 28 (Suppl 1), 2022

Disruption of the Cellular and Extracellular Morphogenesis of Cardiac Tissues in Avian Models of Cyanotic Heart Defects

Richard L. Goodwin[1*], Mohammed K. Khalil[1], Thomas I. Nathaniel[1]

[1]Biomedical Sciences School of Medicine Greenville University of South Carolina, Greenville, SC USA.
* Corresponding author: RLGoodwin@sc.edu

Cyanotic heart defects are a group of congenital structural defects that ultimately result in a lack dermal perfusion, giving skin a bluish (cyan) appearance. These cyanotic defects can have very different etiologies including malformation of the pulmonary veins and the aortic valve, but the most common cyanotic defects involve structural defects in the pulmonary valve. Tetralogy of Fallot (TOF) and Persistent Truncus Arteriosus (PTA) represent opposite end of a spectrum of pulmonary valve defects that cause cyanosis. In TOF the pulmonary valve is either stenotic (too small) or atretic (not formed at all). In PTA, the outflow tract is never divided to the aorta and the pulmonary artery and remains a relatively large, single vessel with multiple valve leaflets. *Gallus gallus* (domestic chicken) models of PTA and TOF have been described previously [1-3]. In this study, we sought to investigate the later stages of fetal heart development in these models when valves tissues have only just begun to deposit elastic and collagen fibers that are critical to valve function [4].

At Hamburger and Hamilton stage 42, chick embryos are approximately, ¾ of the way through gestation and would be analogous to the third trimester of human development, when heart defects become discoverable via ultrasound. PTA hearts were generated using a cardiac neural crest laser ablation protocol developed in Dr Margaret Kirby's lab [1], while TOF hearts were generated using a single application of cyclopamine at HH stage 14 [3]. Pentachrome staining of HH stage 42 cardiac tissues found large scale changes in the cellular and extracellular architecture of the PTA and TOF hearts including the outflow artery diameter (pulmonary artery, aorta, and truncus) and volume, ventricular volume (right and left). Pentachrome staining of pulmonary valve leaflet tissues from PTA and TOF hearts found defect-specific changes to the cellular and extracellular components in comparison to controls (Figure 1). In general, elastic and collagenous fibers were mislocalized throughout the valve leaflet and overall cellularization was affected. The most serval defects were found in the PTA hearts. Analysis of the ultrastructure of these tissues found further evidence of cellular and extracellular dysgenesis (Figure 2).

Determining the structural and ultrastructural pathology that occurs during the development of cyanotic heart defects will aid in the diagnosis and treatment of pulmonary defects. Here, we demonstrate that that two forms of pulmonary defects have two different disease progressions. These different disorders may benefit from specialized interventions that would improve treatment outcomes [5].

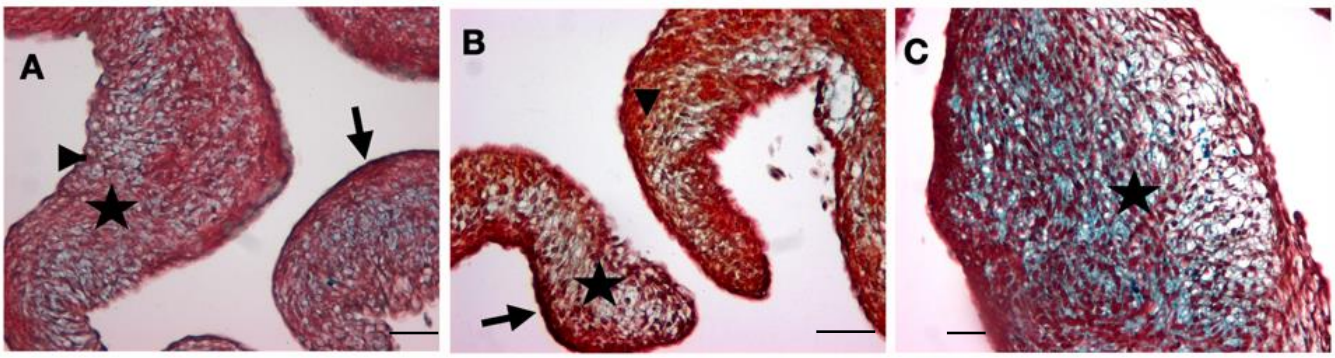

Figure 1. Pentachrome staining of Pulmonary valve leaflets displays cellular and extracellular dysgenesis in avian models Tetralogy of Fallot (TOF) and Persistent Truncus Arteriosus (PTA). Panel A is an image of a control pulmonary leaflet at Hamburger and Hamilton stage 42. Note the elastic fibers (black staining, arrow) in ventricularis, collagen fibers (yellow staining, arrowhead) in corrugated fibrosa, and the ground substance (blue staining, star) of the spongiosa. Panel B shows an analogous pulmonary leaflet in cyclopamine-induced TOF heart. Note the mislocalization of elastic fiber deposition (arrow) in the fibrosa, increase in ground substance and lack of collagen deposition. Also, these leaflets appear to be less cellularized. Panel C shows an analogous outflow leaflet from an avian model of persistent truncus arteriosus generated by ablating cardiac neural crest cells before the septate the outflow tract. These leaflets were highly variable, but had large expansions of the spongiosa and accompanying ground substance. The leaflets presented with dense depositions of elastic and collagenous fibers throughout different regions of the valve leaflet and valve root tissues. Scale bars equal 100 microns.

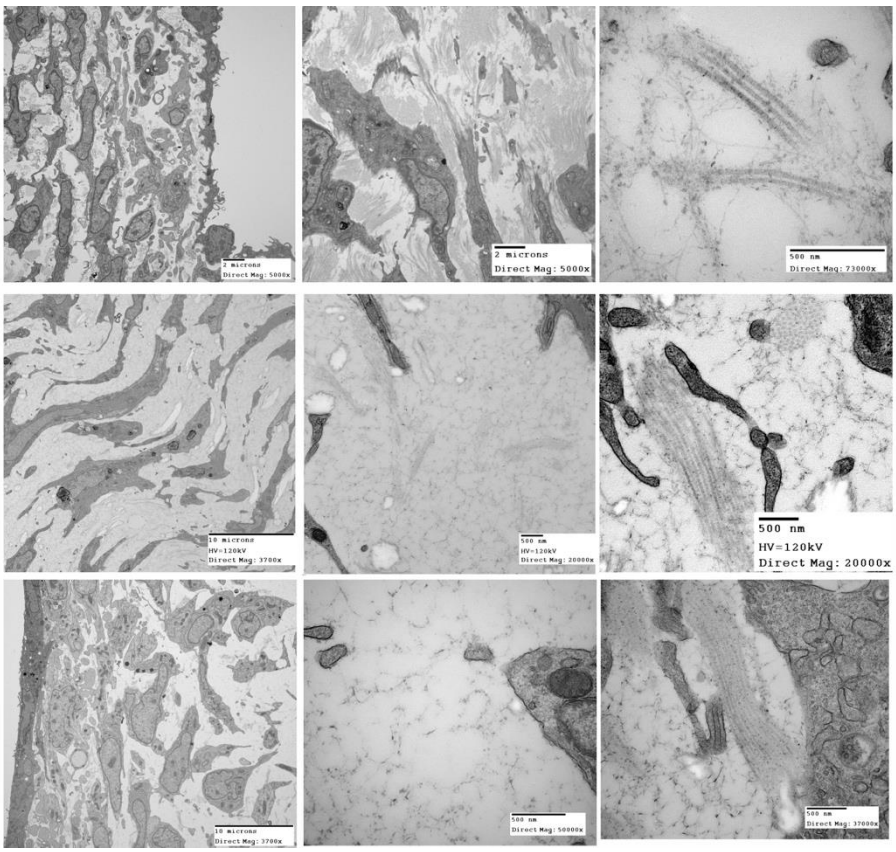

https://doi.org/10.1017/S1431927622005530 Published online by Cambridge University Press

Figure 2. Transmission electron microscopy of valve leaflets show cellular and extracellular dysgenesis in both avian models of TOF and PTA at HH42. The top row shows a series of images of control pulmonary valve leaflets. The left panel shows a view of the valve edge. Note the endothelial cell elaborations of that reach into the lumen of the heart. Developing valve interstitial cells (VICs) also have significant cellular extensions that connect them to each other as well as the basement membrane of the endocardium. The middle panel shows largely isotropic collagen fibers in the valve fibrosa, some of which are closely associated with VIC fibropositor structures. The right panel of this row shows collagen fibers connecting valve mesenchyme to the endocardium. The middle row shows the ultrastructure of pulmonary valve leaflet tissue of a TOF heart. In general, the mesenchyme is less cellularized with more matrix between them (right panel). The extracellular matrix itself appears different with sparse patches of collagen fibers with less organized, smaller diameter fibers, some of which appear to be beaded (middle panel). The right panel shows bundles of collagen fibrils arranged in two distinct originations. The fiber oriented in the plane of the figure (black arrow) displays the "D-period" striations. The fiber oriented into the plane of the figure (black arrowhead) shows the quasi-hexagonal arrangement of collagen fibers in cross-section. In the bottom row, the valve tissue of an outflow leaflet of a PTA heart is shown. The cellular and extracellular matrices of these leaflets were highly variable. However, all had highly cellularized valve margins (left panel) and large amounts of open matrices (middle panel). Regions of dense connective tissue were observed in these leaflets. The right panel shows a fibropositor-like structure in one of these regions.

References:

[1] Besson WT 3rd, et al. Circulation. 1986 Feb;73(2):360-4.
[2] Dyer LA, Kirby ML. Dev Biol. 2009 Jun 15;330(2):305-17.
[3] RS Jones, et al., Microscopy and Microanalysis 23 (S1), 1174-1175. 2017.
[4] RL Goodwin et al., J. Cardiovasc. Dev. Dis., 8(8), 98; 2021.
[5] The authors are grateful for the contributions of Dr Mary Hutson and Jeff Davis to this work.